EFFECTS OF GRAVITY ON SHEARED AND NONSHEARED TURBULENT NONPREMIXED FLAMES

Said Elghobashi, Yong-Yao Lee and Rongbin Zhong

Mechanical and Aerospace Engineering Department
University of California, Irvine, California 92717
Starting Date of Project : July 1994

1 The Problem Considered

The present numerical study is concerned with the fundamental physics of the multi-way interaction between turbulence, chemical reaction and buoyancy in a nonpremixed flame. The method of direct numerical simulation (DNS) is used to solve the instantaneous three-dimensional governing equations. Because of the present supercomputer limitations, we consider two *simple* flow geometries, namely an initially uniform flow without shear (equivalent to grid-generated turbulence) and an initially uniform shear flow. In each flow, the fuel and oxidant initially exist as two separate streams. As the reactants mix, chemical reaction takes place and exothermic energy is released causing variations in density. In the presence of a gravity field, the spatial and temporal distributions of the induced buoyancy forces depend on the local density gradients and the direction of the gravitational acceleration. The effects of buoyancy include the generation of local shear, baroclinic production or destruction of vorticity, and countergradient heat and mass transport. Increased vorticity and small-scale turbulence promote further mixing and reaction. However, if the strain-rates become too high, local flame extinction can occur.
Our **objective** is to gain an understanding of the complex interactions between the physical phenomena involved, with particular attention to the effects of buoyancy on the turbulence structure, flame behavior and factors influencing flame extinction.

2 Mathematical Description

2.1 Approach

We focus our attention to a location in the vicinity of the interface between two initially homogeneous gaseous reactant streams in an unbounded domain. The three-dimensional flow field is initially homogeneous isotropic or sheared turbulence with subsequent development due to density variation arising from chemical energy release and gravitational effects. A schematic of the flow configurations considered is shown in Figure 1. A simple one-step irreversible chemical reaction is considered:

$$\nu_F F + \nu_O O \rightarrow \nu_P P\,, \tag{1}$$

in which two nonpremixed reactants (fuel F and oxidant O) react to form product P. Both finite and infinite reaction rates are considered. In the former, the reaction zone has finite thickness (flamelet), whereas the latter corresponds to the flame sheet approximation. The finite reaction rate is a function of both concentration and temperature. In the case of an infinite reaction rate, a conserved scalar formulation is employed. Transport properties of the fluid such as the mixture dynamic viscosity μ, thermal conductivity K, and mass diffusion coefficient $\rho\mathcal{D}$ are assumed constant for the initial stages of the work. The dependence of these properties on temperature and concentration will be considered later in the study.

2.2 Governing Equations

We consider a low Mach-number turbulent flow with density variations arising from chemical energy release. Thus, the kinetic energy is small in comparison to the thermal energy. Since the time scales of the high frequency acoustic waves are several orders of magnitude smaller than those associated with the convection processes, the former do not interact effectively with the flow dynamics, and thus their effects can be filtered out from the fully compressible equations [6]. The resulting governing equations in nondimensional form are:

$$\frac{\partial \rho}{\partial t} + \nabla \cdot (\rho \boldsymbol{u}) = 0, \tag{2}$$

$$\nabla p^{(0)} = 0, \tag{3}$$

$$\frac{\partial (\rho \boldsymbol{u})}{\partial t} + \nabla \cdot (\rho \boldsymbol{u}\boldsymbol{u}) = -\nabla p^{(1)} - (1/Re)\nabla \cdot \tau + (\rho \boldsymbol{e_k})/Fr, \tag{4}$$

$$\rho \frac{\partial T}{\partial t} + \rho(\boldsymbol{u} \cdot \nabla)T = (1/Pr\ Re)\ \nabla \cdot (\nabla T) + Da\ Ce\ \dot{r}_T, \tag{5}$$

$$\frac{\partial (\rho Y_F)}{\partial t} + \nabla \cdot (\rho \boldsymbol{u} Y_F) = (1/Sc\ Re)\ \nabla \cdot (\nabla Y_F) + Da\ \dot{r}_F, \tag{6}$$

$$\frac{\partial (\rho Y_O)}{\partial t} + \nabla \cdot (\rho \boldsymbol{u} Y_O) = (1/Sc\ Re)\ \nabla \cdot (\nabla Y_O) + Da\ \dot{r}_O, \tag{7}$$

$$\rho = p^{(0)}/T, \tag{8}$$

where standard nomenclature is used and $\boldsymbol{e_k}$ is a unit vector in the gravity direction. The pressures $p^{(0)}$ and $p^{(1)}$ are the (zeroth order) hydrostatic (or thermodynamic) pressure and the (first order) hydrodynamic pressure associated with fluid motion, respectively. In an open domain as considered here $p^{(0)}$ is constant. We also split $p^{(1)}$ into two parts, one is independent of gravity effects and the other equals $(\rho_o\, g\, z)$, thus we have in dimensionless form: $\nabla p^{(1)} = \nabla P + \boldsymbol{e_k}/Fr$.
Equation (4) then becomes:

$$\frac{\partial}{\partial t}(\rho \boldsymbol{u}) + \nabla \cdot (\rho \boldsymbol{u}\boldsymbol{u}) = -\nabla P - (1/Re)\nabla \cdot \tau + [(\rho - 1)\boldsymbol{e_k})]/Fr. \tag{9}$$

The non-dimensional reaction rates are

$$\dot{r}_T = (\rho Y_F)^{\nu_F} (\rho Y_O)^{\nu_O}\ e^{-Ze/T}, \tag{10}$$

$$\dot{r}_i = \frac{W_i(\nu_i'' - \nu_i')}{W_F \nu_F}\ \dot{r}_T. \tag{11}$$

where W_i is the molecular weight of species i and ν_i', ν_i'' are the stoichiometric coefficients for species i existing as reactant and product, respectively. The Reynolds number, Froude number, Prandtl, and Schmidt numbers are defined as

$$\begin{aligned} Re &\equiv \rho_o U_o L_o/\mu_o\ ,\ Fr \equiv U_o{}^2/(L_o\, g)\ , \\ Pr &\equiv \mu_o C_{p_o}/K_o\ ,\ Sc \equiv \mu_o/(\rho_o \mathcal{D}_o)\ , \end{aligned} \tag{12}$$

The subscript 'o' denotes the reference value for the particular quantity. The Damköhler number, defined as the ratio of the convective time to a characteristic chemical reaction time, is given by:

$$Da \equiv (L_o/U_o) \Big/ \left[\frac{W_F \nu_F}{W_F^{\nu_F} W_O^{\nu_O}}\ B\ \rho_o^{(\nu_F + \nu_O - 1)}\right]^{-1}, \tag{13}$$

where B is the pre-exponential coefficient in the dimensional expression for $\dot{r}_T$:

$$\dot{r}_T = (\rho Y_F/W_F)^{\nu_F}\ (\rho Y_O/W_O)^{\nu_O}\ B\, e^{-E_o\,/\,RT}. \tag{14}$$

The non-dimensional energy release parameter and activation energy (Zeldovich number) are:

$$\begin{aligned} Ce &\equiv [h_F^\circ W_F \nu_F + h_O^\circ W_O \nu_O - h_P^\circ W_P \nu_P]/[W_F \nu_F C_{p_o} T_o]\,, \\ Ze &\equiv E_o/RT_o. \end{aligned} \tag{15}$$

In the limit of an infinite reaction rate, the reacting mixture is effectively at chemical equilibrium and the temperature and composition can be determined from a single conserved scalar. In this case, the above energy and species concentration equations are replaced with a single equation for the mixture fraction [8].

2.3 Numerical Procedure

The computational domain considered in the simulations is a finite cube of side length =1. The governing equations are discretized in space using finite differencing except those terms corresponding to the mean advection where a pseudospectral (Fourier) interpolation is used. In general, a finite-difference method requires a larger number of grid points for a given resolution as compared with a fully spectral method. However, the former allows more flexibility in prescribing the boundary conditions. Spatial homogeneity in the horizontal plane allows periodic boundary conditions to be imposed in the $x-$ and $y-$ directions. In the vertical direction, z, a convective outflow boundary condition is employed in order to allow expansion of the flow due to heat release. The simulations are initialized with divergence free velocity fields having random (Gaussian) fluctuations of prescribed correlation spectra. The initial scalar distribution represents two separate streams of (nonpremixed) reactants.
The basic numerical integration scheme follows that of [4]. Integration in time is performed via the Adams-Bashforth scheme. Pressure is treated implicitly and obtained using a Poisson solver. The basic procedure has been used to simulate both decaying isotropic and homogeneous sheared incompressible turbulence ([1] [2] [4] [3] [7]), and an exothermic turbulent nonpremixed reacting flow with zero gravity and infinite rate chemistry [8]. In the present work, further modifications have been made to include *finite rate* chemistry and *nonzero gravity.*

3 Results

Due to the imposed 6-page limit, we present only the results for $Da = \infty$ but with different values of Fr to examine the effects of gravity. As discussed earlier, for the case of $Da = \infty$ we replace equations (5), (6) and (7) with a single equation for the conserved mixture fraction. Distributions of the temperature and mass fractions of all the species are then obtained algebraically from that of the mixture fraction [8]. The results are obtained from a 96^3 mesh and initially homogeneous isotropic turbulence with $Re_{\lambda,o} = 25$, and the nondimensional energy release parameter, Ce, is prescribed such that the ratio $T_{flame}/T_o = 6$. These conditions insure the resolution of the Kolmogorov scale motion throughout the simulation. No mean shear is imposed on the flow. First we discuss the main features of the flow in **zero gravity** ($Fr = \infty$), *the base case,* using the vorticity transport equation :

$$\frac{D\boldsymbol{\omega}}{Dt} = (\boldsymbol{\omega}\cdot\boldsymbol{\nabla})\boldsymbol{u} + \nu\boldsymbol{\nabla}^2\boldsymbol{\omega} - \boldsymbol{\omega}(\boldsymbol{\nabla}\cdot\boldsymbol{u}) + (1/\rho^2)(\boldsymbol{\nabla}\rho\times\boldsymbol{\nabla}p^{(1)}) \; . \tag{16}$$

The four terms on the rhs of Eq. (16) describe, respectively, the rate of change of $\boldsymbol{\omega}$ due to stretching and tilting of the vortex lines, viscous diffusion, velocity divergence due to density variation, and baroclinic torque. In variable density flows, this last term is nonzero only if the density gradient is not aligned with the pressure gradient.
Since no mean shear is imposed on the present flow, both the vorticity and turbulence energy decay due to viscous action. In zero gravity, chemical reaction enhances the rate of vorticity decay in our flow for two reasons. First, the volumetric expansion, $(\boldsymbol{\nabla}\cdot\boldsymbol{u})$, due to the exothermic energy release is positive and thus acts as a sink in Eq. (16). Second, the magnitude of the baroclinic torque near the reaction zone is small since $\boldsymbol{\nabla}p$ and $\boldsymbol{\nabla}\rho$ are nearly aligned parallel to the vertical direction in our flow in which the constant-density surfaces and constant-pressure surfaces are nearly horizontal. The reduction of vorticity in a mixing layer due to non-premixed chemical reaction has been also reported by McMurtry et al. [6] and by Mahalingam et al.[5] in their study of forced, low speed, axisymmetric jet diffusion flame.
The variance of the vorticity is the enstrophy which is completely determined from the turbulence energy spectrum, e.g. for incompressible flow the enstrophy is given by :

$$\omega^2(t)/2 \;=\; D(t)/(2\,\nu) = \int_0^\infty k^2 E(k,t)\,dk, \tag{17}$$

where D is the dissipation rate of the turbulence energy E, and k is the wave number. The transport equation for the enstrophy is

$$\frac{D(\omega^2/2)}{Dt} = (\boldsymbol{\omega}\cdot S\cdot\boldsymbol{\omega}) + \nu\nabla^2(\omega^2/2) - \nu\nabla\boldsymbol{\omega} : (\nabla\boldsymbol{\omega})^T - \omega^2(\nabla\cdot\boldsymbol{u}) + (1/\rho^2)\boldsymbol{\omega}\cdot(\nabla\rho\times\nabla p^{(1)}) \ , \quad (18)$$

where S is the rate of strain tensor. The terms on the rhs of Eq. (18) describe the rate of change of $(\omega^2/2)$ due to, respectively, vortex stretching or tilting, viscous diffusion, viscous dissipation, velocity divergence and baroclinic torque. It is seen that the velocity divergence and baroclinic torque have the same effect on the enstrophy as on the vorticity. Reducing the enstrophy means reducing the turbulence energy, E, and its dissipation rate, D. Reduction of D results in *increasing* the Kolmogorov scale, η, and hence a reduction of scalar gradients, scalar mixing and thus the reaction rate [8].

Simulations for **nonzero gravity** with two values of Fr (17.6 and 7.04) were performed.
Our results indicate that the baroclinic torque near the reaction zone increases with increasing the gravitational acceleration (i.e. reducing Fr). The evidence is clear both in the physical space results (contours of temperature, velocity and vorticity) and in the wave-number space (spectra of $E(k)$ and $D(k)$).
In the reaction zone, the buoyancy force causes hot products to rise in the $z-$ direction and lower-temperature-fuel to move downwards toward the reaction zone. This is observed via the instantaneous contours of the $w-$ velocity and temperature in any vertical (xz) plane. Thus alternating 'hot' and 'cold' fluid parcels cross the horizontal planes in the neighborhood of the reaction zone. A strong density gradient is thus established in the horizontal (x,y) directions in addition to that in the vertical direction. Accordingly $\nabla\rho$ and ∇p become misaligned thus increasing the magnitude of the baroclinic torque, the vorticity and the enstrophy. The instantaneous contours of ω_y show that it attains its maximum magnitude near the flame but it changes its sign across the reaction zone. The presence of the reaction zone between opposite-sign vorticities has been also observed by Mahalingam et al.[5] in their study of forced, low speed, buoyant axisymmetric jet diffusion flame.
Now we discuss the effect of buoyancy on the spectra of turbulence energy. Since the reacting flow is inhomogeneous in the z-direction, we can examine the spectra in horizontal planes. Figure 2 shows the spectra of the $z-$component of energy, $E_3(k)$, at times t=2 and t=5 and $x-$ component of energy, $E_1(k)$, at t=5, for $Fr = \infty, 17.6, 7.04$ on the plane $z = 0.5$ which is the initial interface between fuel and oxidant streams. It is seen that $E_3(k)$ decreases with time for the zero-gravity case, $Fr = \infty$, as explained earlier. In contrast, the energy and dissipation (not shown) increase with lowering Fr, thus reducing the Kolmogorov length scale and increasing the integral length scale, i.e. increasing the turbulence Reynolds number. The result is a reduction of the thickness of the reaction zone and an increase of its surface area due to wrinkling, hence an increase of the total consumption rate of the reactants. The increase of energy occurs first in $E_3(k)$ at high wave numbers (Fig. 2) where chemical reaction takes place, then due to thermal diffusion all scales become affected as time increases. The transfer of turbulence energy from $E_3(k)$ to both $E_1(k)$ and $E_2(k)$ occurs via the pressure-strain interactions. The anistropy of turbulence is seen in Fig.2 by comparing $E_3(k)$ and $E_1(k)$ at t=5. We also examined the balance of energy in the Fourier space:

$$dE(k)/dt = T(k) + G(k) + P(k) - D(k) \ , \quad (19)$$

where the four terms on the rhs describe respectively the nonlinear transfer of energy in a given coordinate direction between the different scales, the transfer from potential to kinetic energy, the transfer of energy due to pressure gradients and the viscous dissipation. The time behavior of $G(k)$ shows that initially high wave numbers (small scales) are the first to be affected by gravity, and in time the peak of $G(k)$ shifts gradually to lower wavenumbers (larger scales). Also $G(k)$ is larger by at least an order of magnitude than the other terms on the rhs of Eq. (19) and increases monotonically as expected.

4 Future Work

The following phenomena will be studied in a stepwise manner during the next 3 years : 1) chemical kinetics for finite values of Da and examination of flame extinction in a range of values of Fr, Re_λ ; 2) uniform mean shear ; 3)varying the direction of the gravity vector relative to the F/O interface plane (normal or parallel) ; 4) dependence of fluid properties on temperature.

References

[1] S.E. Elghobashi, T. Gerz, and U. Schumann. Direct simulation of turbulent homogeneous shear flow with buoyancy. *Fifth International Symposium on Turbulent Shear Flows, Cornell Univ.*, pages 227–233, 1985.

[2] S.E. Elghobashi, T. Gerz, and U. Schumann. Direct simulation of the initial development and the homogeneous limit of the thermal mixing layer. *Sixth International Symposium on Turbulent Shear Flows, Toulouse, France*, pages 511–516, 1987.

[3] S.E. Elghobashi and K.K. Nomura. Direct simulation of a passive diffusion flame in sheared and unsheared homogeneous turbulence. *Turbulent Shear Flows, Springer-Verlag, W.C. Reynolds, ed.*, 7:313–329, 1990.

[4] T. Gerz, U. Schumann, and S. Elghobashi. Direct simulation of stably stratified homogeneous turbulent shear flows. *J. Fluid Mech.*, 200:563–594, 1989.

[5] S. Mahalingam, B.J. Cantwell, and J. H. Ferziger. Full numerical simulation of coflowing axisymmetric jet diffusion flames. *Phys. Fluids*, A2:720–728, 1990.

[6] P. A. McMurtry, J. J. Riley, and R. W. Metcalfe. Effects of heat release on the large-scale structure in turbulent mixing layers. *J. Fluid Mech.*, 199:297–332, 1989.

[7] K.K. Nomura and S.E. Elghobashi. Mixing characteristics of an inhomogeneous scalar in isotropic and homogeneous sheared turbulence. *Phys. Fluids*, 4:606–625, 1992.

[8] K.K. Nomura and S.E. Elghobashi. The structure of inhomogeneous turbulence in variable density nonpremixed flames. *Theoretical and Computational Fluid Dynamics*, 5:153–175, 1993.

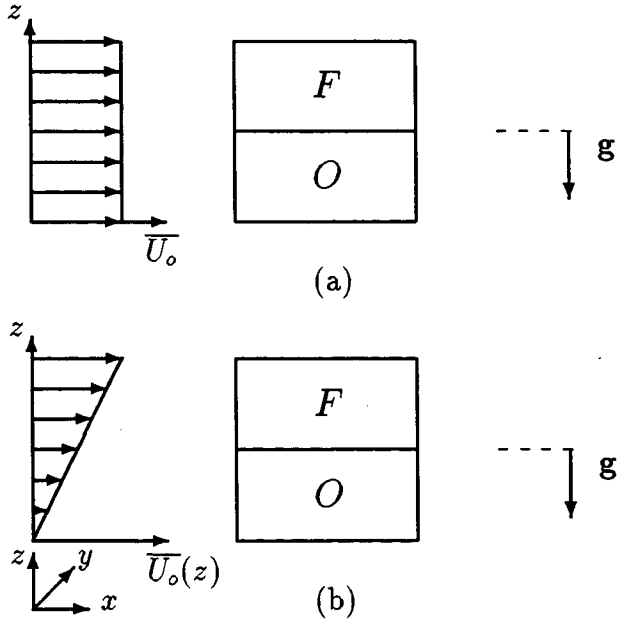

Figure 1: Schematic of flow configurations: (a) uniform mean velocity; (b) uniform mean velocity gradient in $z-$direction. The direction of the gravity vector may be either parallel or perpendicular to the initial interface between the fuel (F) and the oxidant (O), thus simulating a horizontal or vertical flame.

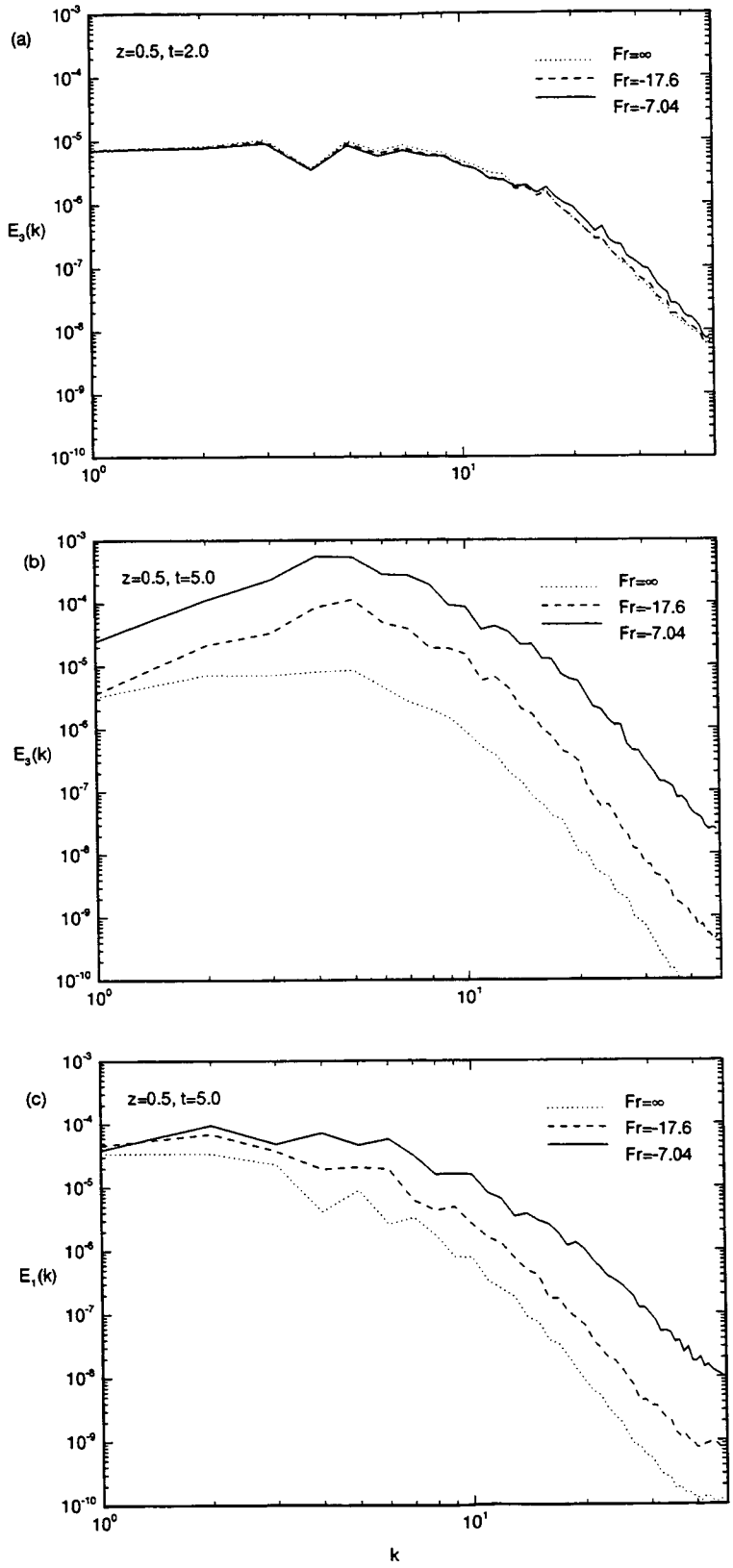

Figure 2: Spectra of turbulence energy components $E_3(k)$ and $E_1(k)$ on a horizontal plane (z=0.5) for different Fr.